Manipulation of polar order in the "empty" tetragonal tungsten bronzes: $Ba_{4-x}Sr_xDy_{0.67}\square_{1.33}Nb_{10}O_{30}$, x = 0, 0.25, 0.5, 1, 2, 3

Jonathan Gardner[1], Finlay D. Morrison[1]*

[1]EaStCHEM School of Chemistry, University of St Andrews, North Haugh, St Andrews, KY16 9ST, UK

Abstract

A series of "empty" tetragonal tungsten bronze (TTB) ferroelectrics, $Ba_{4-x}Sr_xDy_{0.67}\square_{1.33}Nb_{10}O_{30}$, ($x$ = 0, 0.25, 0.5, 1, 2, 3; $\square$ = vacancy), is reported. With increasing x the unit cell contracts in both the *ab* plane and *c*-axis; $x \leq 1$ compounds are normal ferroelectrics (FE) with decreasing T_C as x increases, while $x \geq 2$ are relaxor ferroelectrics (RFE) with associated frequency dependent permittivity peaks and with similar T_m and T_f (Vogel-Fulcher freezing temperatures) values. This observation is rationalised by differing cation occupancies: for $x \leq 1$, Sr^{2+} principally occupies the A2-site (co-occupied by Ba^{2+} with the A1-site occupied by Dy^{3+} and vacancies); for x $\geq$ 2 significant Sr A1-site occupation leads to the observed RFE characteristics. This FE to RFE crossover is consistent with a previously proposed TTB crystal chemical framework where both a decrease in average A-site size and concurrent increase in A1-site tolerance factor (t_{A1}) favour destabilization of long range polar order and relaxor behaviour. The effect of increasing t_{A1} as a result of Sr occupancy at the A1 site is dominant in the compounds reported here.

Tetragonal tungsten bronze oxides (TTBs) are perovskite-related structures, general formula $A1_2A2_4B1_2B2_8C_4O_{30}$. The TTB structure is derived from the corner-sharing BO_6 perovskite network by rotation of alternate "perovskite columns" in the c-axis which breaks the degeneracy of the A-sites to form the additional A2- and C-sites associated with the pentagonal and trigonal TTB-channels. The retained perovskite-like A1-sites and larger A2-sites are typically occupied by cations of large radius (*e.g.* Ba^{2+}, Na^{+}, Gd^{3+}) while the small C-site accommodates only small cations (*e.g.* Li^{+}) and in the majority of TTBs these are unoccupied. TTBs exhibit a wide range of stoichiometry as a result of varying A-site occupancy and as a result are variously described as: "filled" where all the A-sites are fully occupied (*e.g.* $Ba_4Na_2Nb_{10}O_{30}$); "unfilled" with typically 5/6 or greater A-site occupation *e.g.* SBN, $(Sr,Ba)_5Nb_{10}O_{30}$); or "empty" where <50% A1-site occupancy is present.[1] TTBs variously display a range of ferroelectric, relaxor and relaxor-ferroelectric properties due to complex structure-property inter-relationships related to commensurately and incommensurately modulated super-structures and resulting polar order over varying lengths scales. Building on work by Zhu et al[2] the A-cation size difference was shown to be an important parameter, we recently proposed a more-detailed crystal-chemical framework which relates the overall average A-site cation size and tolerance factor at the A1-site with the predicted nature of polar ordering (ferroelectric vs relaxor) and structural modulations (commensurate vs incommensurate).[1] By this crystal-chemical model, the (isovalent) substitution of Sr^{2+} (r = 1.50 Å for CN 15) by larger Ba^{2+} (r = 1.65 Å for CN 15) at the A2-site increases the average A-site size leading to stabilization of polar order as observed in filled $(Ba,Sr)_4R_2Ti_4Nb_6O_{30}$ TTBs and unfilled SBN.[2,3] We have previously reported a number of "empty" TTBs compounds, $Ba_4R_{0.67}\square_{1.33}Nb_{10}O_{30}$, (R = La, Nd, Sm, Gd, Dy and Y, and $\square$ = vacancy) which conform to this framework with a crossover from relaxor-ferroelectric (R =

La) to normal ferroelectric (R = Nd, Sm, Gd, Dy and Y) with decreasing A1-cation size, but show more complex structural behaviour due to effect of vacancies.[1,4,5] In this contribution, starting from the normal ferroelectric $Ba_4Dy_{0.67}\square_{1.33}Nb_{10}O_{30}$ (T_C = 524 K) we show that successive replacement of Ba^{2+} with Sr^{2+} ($Ba_{4-x}Sr_xDy_{0.67}\square_{1.33}Nb_{10}O_{30}$, x = 0, 0.25, 0.5, 1, 2, 3) destabilises long range polar ordering, leading to a decrease in T_C and onset of relaxor ferroelectric behaviour in line with the predictions of the recent crystal-chemical model.[1]

All compounds were produced using a standard solid-state method; a detailed procedure for the x = 0 composition has been reported previously.[4] Strontium compounds (x > 0) were prepared from $BaCO_3$, $SrCO_3$, Nb_2O_5, and Dy_2O_3 (Aldrich, all > 98+ % purity) precursor powders and heated to 1000 ˚C for 2 hours, then 1250 ˚C for 15 hours followed by milling, pressing into pellets and sintering at 1350 °C for 12 hours. Additional milling and heating (1350 °C for 12 hours) was required to yield dense (> 90% theoretical density) single phase ceramics. Powder X-ray diffraction (PXRD) data were collected using a PANalytical Empyrean diffractometer. Dielectric measurements were performed with Agilent 4294A and Wayne Kerr 6500B impedance analysers with the sample mounted in a closed cycle cryocooler or tube furnace. Polarization-electric field (*P*-*E*) data were measured using an aixACCT TF2000 Analyzer.

PXRD data of all compositions may be indexed to a simple TTB structure with tetragonal symmetry. For x = 3, small amounts of the Fergusonite-type phase, $DyNbO_4$,[6] was detected despite additional milling and sintering steps. The $DyNbO_4$ was estimated to be of 2% phase fraction and 1.4 % weight fraction by Rietveld refinement using a simple tetragonal space group (*P*4*bm*) and the $DyNbO_4$ structural model of Keller.[6] No additional peaks were observed and while some high angle peaks appeared to be slightly broadened it was not of a sufficient extent to assign lower symmetry. This is consistent with our previous report of $Ba_4R_{0.67}\square_{1.33}Nb_{10}O_{30}$, (R = La, Nd, Sm, Gd, Dy and Y) compounds[4] which also appear

metrically tetragonal using laboratory PXRD. Distortions of lower symmetry observed in TTBs (including the $Ba_4R_{0.67}\square_{1.33}Nb_{10}O_{30}$ compounds) are typically very subtle[5] with superstructures derived from modulations of the oxygen sublattice, which require study using high resolution diffraction techniques.[1,5] For Rietveld refinements the occupancy across all sites was constrained to match the nominal overall stoichiometry but various starting points were then employed to ensure refinements were not converging on a local minimum; site occupancies consistently resulted in sole A2 occupancy for Ba and A1 for Dy. For Sr-containing compositions refinements were also carried out with Ba constrained to the A2 site and Dy to A1 with Sr occupancy varying across A2 and A1, ranging from maximum Sr content on A1 to all on A2; these approaches all resulted in the same final occupancies. For x = 3, adjustment of the TTB composition (0.63 Dy at the A1 site) to compensate for the small amount of observed $DyNbO_4$ second phase had negligible effect on the final ratio of Ba:Sr:Dy occupancies across the A-sites.

The lattice parameters decrease with increasing x, with a greater effect observed for $x \geq 1$, Table I. This is consistent with solid solutions in which Ba^{2+} is replaced by Sr^{2+} and also with the typically smaller c values reported for Sr-based TTBs.[2] Refined occupancies of Sr^{2+} at the A-sites indicate little or no Sr^{2+} A1-site occupation for $x \leq 1$, but increased significant for $x >$ 1 (discussed later). Dielectric data for x = 0 exhibits a single frequency independent peak in the permittivity corresponding to the ferroelectric Curie temperature, T_C. With increasing x, T_C decreases, Figure 1, together with a simultaneous broadening of the peak, until a low temperature relaxor-like peak with large frequency dependence is observed for x = 2 and 3, Figure 2. Within this series, crystal anisotropy (measured by tetragonality, c/a) correlates with T_C, Table I, as reported for $Ba_4R_{0.67}\square_{1.33}Nb_{10}O_{30}$, (R = La, Nd, Sm, Gd, Dy and Y) compounds.[4] The most intense peaks in the dielectric loss (tan δ) data, Figure 1, associated with T_C, behave similarly. Additionally, $0 \leq x \leq 1$ have multiple very weak and broad

anomalies at low temperatures, extending approximately between 50-100 K and 250-350 K, in addition to the ferroelectric transition. Similar low temperature relaxations are commonly observed to varying degrees in TTBs and have been attributed to: low temperature phase transitions or subtle structural modifications without symmetry change;[8] octahedral tilting;[9] incommensurate modulations[10-12] (more specifically small changes to the incommensurate modulation[13]); freezing-out of polarisability/polarisation fluctuations in the *ab* plane;[14] and frustrated ferroelectric-ferroelastic transitions.[15] In single crystal studies of doped (Sr-rich) SBN TTBs, dielectric data measured along the *c*-axis is dominated by the high temperature ferroelectric-paraelectric phase transition, whereas in the *ab* plane low temperature anomalies dominate.[16,17] Variable-temperature structural investigation using synchrotron PXRD (down to 100 K) or PND (down to 20 K) of the related "empty" TTB $Ba_4La_{0.67}\square_{1.33}Nb_{10}O_{30}$ which exhibits complex relaxor-ferroelectric behaviour[5], showed no evidence for a low temperature phase transition, either at temperatures corresponding to the principal relaxor peak (T_m at 297 K for 1 MHz) or lower. These low temperature anomalies are not evident in the permittivity for low concentrations of Sr^{2+} dopant, however, for x =1, Figure 2a, in addition to the main peak, a weak frequency dispersion (referred to as a "shoulder" in the literature[18]), extends over the temperature range corresponding to the relaxor peaks in x = 2 and x = 3, Figure 2b.

Both x = 2 and 3 exhibit low temperature relaxor-like properties with a characteristic increase in peak maximum temperature, T_m, with increasing frequency in both the relative permittivity, Figure 2, and dielectric loss. Although x = 2 has a larger permittivity at T_m, both compounds exhibit a similar degree of relaxor behaviour with comparable T_m values and degrees of frequency dispersion. This was examined more quantitatively by modelling the frequency dependence of the permittivity using the Vogel-Fulcher expression:

$$f = f_0 \exp\left(-\frac{E_a}{k(T_m - T_f)}\right)$$

where f is the frequency of the applied ac field, f_0 is the limiting response frequency, E_a is the activation energy, k is Boltzmann's constant and T_m is the maximum of the relative permittivity measured with ac field of frequency, f.[19-21] The polarisation freezes out at T_f, the static freezing temperature, also known as the Vogel-Fulcher temperature.[19,20] Data for both x = 2 and x = 3 are well represented by Vogel-Fulcher relationship and the values obtained for the fitting parameters (for x = 2, E_a = 0.12 eV, $f_0 = 1.23\times 10^{10}$ Hz and T_f = 165 K; for x = 3, , E_a = 0.16 eV, $f_0 = 2.28 \times 10^{11}$ Hz and T_f = 159 K) are physically realistic and comparable to values reported for other TTBs.[2,20] The similarity of T_m and T_f values is likely to originate from site occupancy differences. If the A-cations were ordered based on size differences, irrespective of x, with the larger Sr^{2+} and Ba^{2+} cations solely occupying the A2-site and Dy^{3+} the A1-site the average A-cation size would decrease with increasing Sr but the A1-site tolerance factor (t_{A1}) would remain unchanged. This would represent a vertical displacement on Figure 17 of Ref 1, and so, based on our crystal-chemical model and Chen and co-workers size difference argument, one would therefore expect a decrease in stability of long range polar (decrease in T_C or T_m/T_f) and an increase in the degree of relaxor-type character with increasing x based simply on the reduced average A-cation size reducing B-site displacements.

Rietveld refinements of PXRD data for $x \geq 2$ indicate an increased degree of Sr occupancy at both A2 and A1 sites, relative to lower values of x. However, x = 2 has a relatively higher proportion of Sr_{A1} occupancy (Sr_{A1} = 0.5116, Sr_{A2} = 1.4884; Sr_{A1}/Sr_{A2} = 0.34) compared to x = 3 (Sr_{A1} = 0.4348, Sr_{A2} = 2.6176; Sr_{A1}/Sr_{A2} = 0.17). The higher Sr_{A1} for x = 2 may explain the similarity of the observed dielectric properties despite the compositional difference. Higher occupancy of Sr on the A1-site leads to an increased t_{A1} tolerance factor for x = 2, such that $t_{A1\ (x\ =\ 2)} > t_{A1\ (x\ =\ 3)}$, Table 1. This multi-site occupancy by Sr generates two contributing factors which favour relaxor behaviour: 1) A-site disorder; and 2) reduced

octahedral tilting due to the increase in A1-cation size (increased t_{A1}). In order to understand which is dominant one can consider the role played by disorder in the related filled TTB compositions $Ba_4R_2Ti_4Nb_6O_{30}$ and $Ba_5RTi_3Nb_7O_{30}$ where R = La, Nd.[14] In the Ba_4R_2 compositions Ba and R solely occupy A2 and A1 sites, respectively, whereas the Ba_5R analogues necessarily have A1-site disorder. Despite having the same degree of occupational A1 disorder $Ba_5LaTi_3Nb_7O_{30}$ displays a higher degree of relaxor behaviour than $Ba_5NdTi_3Nb_7O_{30}$; the influence on tilting by change in the A1 cation size and hence t_{A1} is clearly dominant in these compositions. The large change in t_{A1} in the $x \geq 2$ compositions here is also likely to dominate; the increase in t_{A1} frustrates oxygen octahedral tilting resulting in increased relaxor behaviour as also observed in Sr rich SBN compounds where Sr occupies both A-sites.[3,22]

Polarisation-electric field (P-E) data for x = 0.25, Figure 3(a), display normal, saturated ferroelectric P-E loops and associated switching current. For $x \leq 1$, normal P-E loops are recorded up to 473 K, with the coercive field decreasing with increasing temperature as expected. x = 0.25 exhibits normal ferroelectric loops initially, however, after a large number of cycles (> 50) at elevated temperature (413 K) the P-E loop slowly distorts leading to a asymmetric loops, Figure 3 (b), which are morphologically similar to those previously observed in some poled hard PZTs.[23] The asymmetry increases with successive cycling and the rate of loop distortion increases greatly with the magnitude of the applied field and elevated temperature; the effect is comparably negligible at ambient temperature. A sample orientation effect also exists; reversing the direction of the bipolar excitation signal (or by simply turning the sample over) reduces the asymmetry initially, before re-developing the same asymmetry in the opposite bias direction. Annealing at high temperature (*e.g.* 623 K) while the sample is electrically shorted regenerates the initial symmetrical loop at ambient temperature. The behaviour observed here occurs upon application of a sequence of 4 bipolar

excitation cycles, each with a positive (P) and negative (N) triangular waveform (PNPNNPNP). This may be related to the relaxation time with the successive negative (and non-switching) resulting in a net unipolar effect. This was confirmed by means of standard P-E loops recorded using the PNP**NN**PNP pulse sequence but systematically varying the time between subsequent pulse sequences (measurements). Short times between measurements produced little loop distortion or reduced distortion in a sample in which the asymmetric loop had been previously established, i.e. this has a similar effect as a symmetrical PNPNPN… sequence. This is unsurprising as successive PNP**NN**PNP pulses applied with intervals comparable those within the pulse sequence result in PNP**NN**PN**P P**NP**NN**PNP… sequence. Increasing the interval between PNP**NN**PNP pulses increases the distortion effect. The key factor is the interval experienced by the sample between the reinforcing NN in the middle of the pulse chain and the PP in subsequent (separate) pulses. This chronologically asymmetric field history results in distorted P-E loops displaced in the polarisation axis due to charge accumulation under the electrode,[24] most likely due to oxygen vacancy migration.

For $x \geq 2$, below the respective relaxor peak, P-E loops are slim and not well saturated with broad switching current peaks, Figure 3 (c), becoming slimmer with increasing temperature, *i.e.*, behaviour characteristic of relaxors[25], Figure 3 (d). Due to the rapid increase in coercive field with decreasing temperature we were unable to obtain saturated loops at much lower temperatures, unlike other "empty" TTBs such as $Ba_4La_{0.67}\square_{1.33}Nb_{10}O_{30}$.[4,5] However, such large temperature dependences of coercive field are not uncommon in RFEs.[26]

Within the series of compounds reported here, similarities to well studied SBN allow us to identify number of contributions to crossover behaviour observed with increasing x: increase in A2 vacancies for $x \geq 2$ compounds which has been reported as favouring relaxor behaviour.[27] An increase in disorder across A1- and A2-sites[28] and change in average A-

cation size within both the A1- and A2-sites favour relaxor behaviour and is consistent with the crystal-chemical model.

Based on initial refinements, Ba^{2+}, Sr^{2+} and vacancies occupy the A2-site while the A1-site has additional charge disorder due to occupation by both Sr^{2+} and Dy^{3+} as well as vacancies. Cation disorder is favorable to onset of relaxor behaviour,[28,29] however as discussed previously is unlikely to be the dominant influence within this particular system.

The additional effect of vacancies is also expected here. The effect of vacancies is difficult to precisely interpret, although some work has been done on perovskites,[30] however they may have a large impact on the structural and dielectric properties of TTBs.[1,27,31,32]

By the crystal-chemical model, the (isovalent) substitution of Ba^{2+} by smaller Sr^{2+} decreases the overall A-site size (A1+A2)/2 and reduce the "stretching" effect in the c-axis, reducing the likelihood of long-range polar ordering. Altered cation occupation of the A-sites (with site preference dependent on A-cation size difference) changes the average A1-cation size and therefore t_{A1}; this strongly influences ferroelectric *vs.* relaxor behaviour due to the resulting tilt system.[1,14,33] In the compositions reported here direct replacement of Ba by Sr solely on the A2-site would reduce the average A-cation size ((A1+A2)/2) with increasing x while t_{A1} remains constant. However, Sr occupancy at the A1-site for $x \geq 2$, as determined from PXRD data, significantly increases the average A1-site size and t_{A1}. Based on the crystal-chemical model this drives onset of relaxor behaviour as shown in Fig 17 in ref 1.

Decreasing the A2-site size with increasing x reduces the c-axis 'stretch' leading to shortening of O-Nb-O bonds and concomitant reduction in t_{A1} which induces frustrated tilting favouring relaxor properties. However, when considered alongside other TTBs it appears that the effect on tilting controlled by t_{A1} is dominant in determining cross-over from "normal" ferroelectric to relaxor behaviour.

Acknowledgements

JG would like to thank the EPSRC for provision of a studentship *via* the doctoral training grant (EP/K503162/1). The research data supporting this publication can be accessed at DOI: 10.17630/534de52f-0b19-41b9-bde8-0218138c29c0

[1] X. Zhu, M. Fu, M. C. Stennett, P. M. Vilarinho, I. Levin, C. A. Randall, J. Gardner, F. D. Morrison, and I. M. Reaney, Chem. Mater. **27**, 3250 (2015).
[2] X. L. Zhu, S. Y. Wu, and X. M. Chen, Appl. Phys. Lett. **91**, 162906 (2007).
[3] A. M. Glass, J. Appl. Phys. **40**, 4699 (1969).
[4] J. Gardner and F. D. Morrison, Dalton Trans. **43**, 11687 (2014).
[5] J. Gardner, F. Yu, C. Tang, W. Kockelmann, W. Zhou, and F.D. Morrison, Chem. Mater. **28**, 4616 (2016).
[6] C. Keller, *Z. anorg. allg. Chem.,* **318**, 89 (1962).
[7] R. D. Shannon, Acta Crystallogr. A,. **32**, 751 (1976).
[8] Y. H. Xu, Z. G. Li, W. Li, H. Wang, and H. C. Chen, Phys. Rev. B. **40**, 11902 (1989).
[9] J. H. Ko, F. Jiang, and S. Kojima, Ferroelectrics **270**, 1395 (2002).
[10] M. Venet, J. C. M'Peko, F. L. Zabotto, F. Guerrero, D. Garcia, and J. A. Eiras, Appl. Phys. Lett. **94**, 172901 (2009).
[11] H. Q. Fan, L. Y. Zhang, and X. Yao, J. Mater. Sci. **33**, 895 (1998).
[12] S. M. Ke, H. Q. Fan, H. T. Huang, H. L. W. Chan, and S. H. Yu, J. Appl. Phys. **104**, 024101 (2008).
[13] J. Schefer, D. Schaniel, V. Pomjakushin, U. Stuhr, V. Petricek, T. Woike, M. Wohlecke, and M. Imlau, Phys. Rev. B. **74**, 134103 (2006).
[14] X. L. Zhu, K. Li, and X. M. Chen, J. Am. Ceram. Soc. **97**, 329 (2014).
[15] A. Torres-Pardo, R. Jimenez, J. M. Gonzalez-Calbet, and E. Garcia-Gonzalez, Inorg. Chem. **50**, 12091 (2011).
[16] J. H. Ko, S. Kojima, S. G. Lushnikov, R. S. Katiyar, T. H. Kim, and J. H. Ro, J. Appl. Phys. **92**, 1536 (2002).
[17] I. A. Santos, D. U. Spinola, D. Garcia, J. A. Eiras, E. R. Manoel, A. C. Hernandes, J. A. G. Carrio, and Y. P. Mascarenhas, Ferroelectrics **238**, 711 (2000).
[18] X.L. Zhu, X. Q. Liu, and X. M. Chen, J. Am. Ceram. Soc. **94**, 1829 (2011).
[19] D. Viehland, S. J. Jang, L. E. Cross, and M. Wuttig, J. Appl. Phys. **68**, 2916 (1990).
[20] A. Rotaru, D. C. Arnold, A. Daoud-Aladine, and F. D. Morrison, Phys. Rev. B. **83**, 184302 (2011).
[21] A. Rotaru and F. D. Morrison, J. Therm. Anal. Calorim. **120**, 1249 (2015).
[22] G. H. Olsen, U. Aschauer, N. A. Spaldin, S. M. Selbach, and T. Grande, Phys. Rev. B. **93**, 180101 (2016).
[23] T.R. Shrout and S.J. Zhang, J. Electroceram. **19**, 113 (2007).
[24] J. F. Scott, *Ferroelectric Memories*. (Springer-Verlag, Berlin 2000), page 2.
[25] L. Jin, F. Li, and S. J. Zhang, J. Am. Ceram. Soc. **97**, 1 (2014).
[26] I. W. Chen and Y. Wang, Ferroelectrics **206**, 245 (1998).
[27] T. Wei, Z. Dong, C. Z. Zhao, Y. Y. Guo, Q. J. Zhou, and Z. P. Li, J. Appl. Phys. **119**, 124107 (2016).
[28] V. Hornebecq, C. Elissalde, F. Weill, A. Villesuzanne, M. Menetrier, and J. Ravez, J. Appl. Crystallogr. **33**, 1037 (2000).
[29] J. Schefer, D. Schaniel, V. Petříček, T. Woike, A. Cousson, and M. Wöhlecke, Z. Kristallogr. **223**, 399 (2008).
[30] R. Ubic, K. Tolman, K. Chan, N. Lundy, S. Letourneau, and W. M. Kriven, J. Alloys Compd. **575**, 239 (2013).
[31] A. Belous, O. V'yunov, D. Mishchuk, S. Kamba, and D. Nuzhnyy, J. Appl. Phys. **102**, 014111 (2007).
[32] X. Y. Xiao, Y. Xu, Z. G. Zeng, Z. L. Gui, L. T. Li, and X. W. Zhang, J. Mater. Res. **11**, 2302 (1996).

[33] C. J. Huang, K. Li, X. Q. Liu, X. L. Zhu, and X. M. Chen, J. Am. Ceram. Soc. **97**, 507 (2014).

Table I – Lattice parameters, unit cell volume, tetragonality (c/a)[†], $A1B2O_3$ tolerance factors (t_{A1})[‡] obtained from PXRD data and T_C[a] or T_m[b] values (at 1 MHz) determined dielectric data for $Ba_{4-x}Sr_xDy_{0.67}Nb_{10}O_{30}$.

x	***a* (Å)**	***c* (Å)**	***V* (Å^3)**	***c*/*a***	t_{A1}	T_C ***or*** T_m **(K)**
0	12.4585(6)	3.9543(6)	613.76(2)	0.3174	0.900	523[a]
0.25	12.4584(7)	3.9579(4)	614.31(7)	0.3177	0.909	516[a]
0.5	12.4549(9)	3.9536(4)	613.31(9)	0.3174	0.905	500[a]
1	12.4566(6)	3.9499(3)	612.89(6)	0.3171	0.901	469[a]
2	12.4361(5)	3.9103(2)	604.75(5)	0.3144	0.941	314[b]
3	12.3900(5)	3.8852(2)	596.42(5)	0.3136	0.937	298[b]

[†] Numbers in parentheses indicate standard deviations of the refined parameters, in units of the least-significant figures, as estimated in the GSAS software.
[‡] Calculated based on the following (12 coordinate) ionic radii[7]: r_{Sr} = 1.44 Å; r_{Dy} = 1.175 Å.

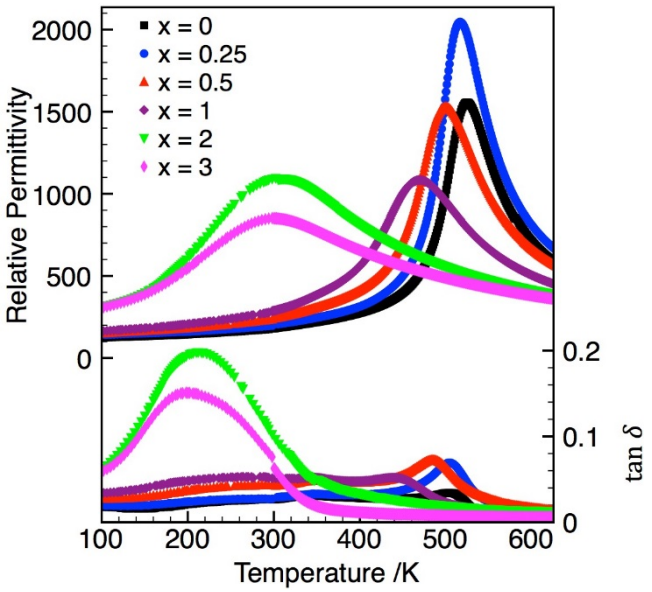

Figure 1. Relative permittivity, ε', and dielectric loss, tan δ, data (at 1 MHz) as a function of temperature for $Ba_{4-x}Sr_xDy_{0.67}Nb_{10}O_{30}$ (x = 0, 0.25, 0.5, 1, 2, 3).

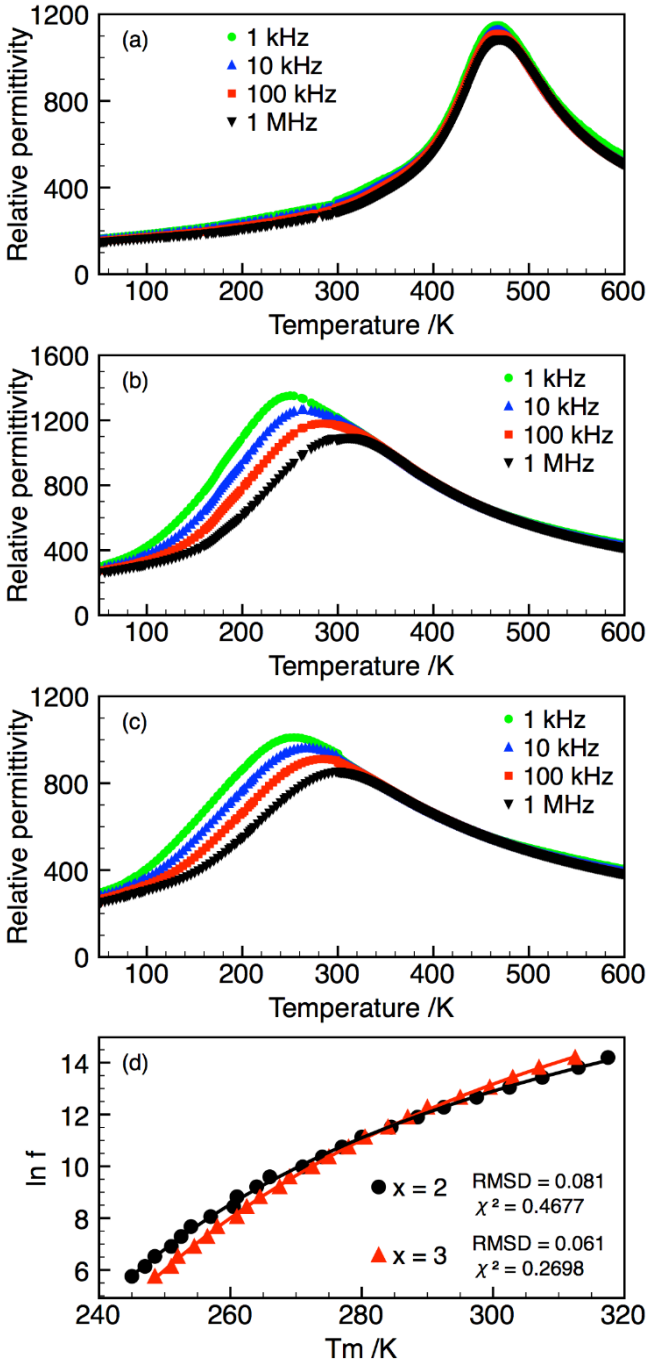

Figure 2. Relative permittivity data for $Ba_{4-x}Sr_xDy_{0.67}Nb_{10}O_{30}$, (a) $x = 1$, (b) $x = 2$, (c) $x = 3$ at selected frequencies and (d) Vogel-Fulcher fits for $x = 2$ and 3 including goodness-of-fit parameters (root mean square standard deviation and χ^2).

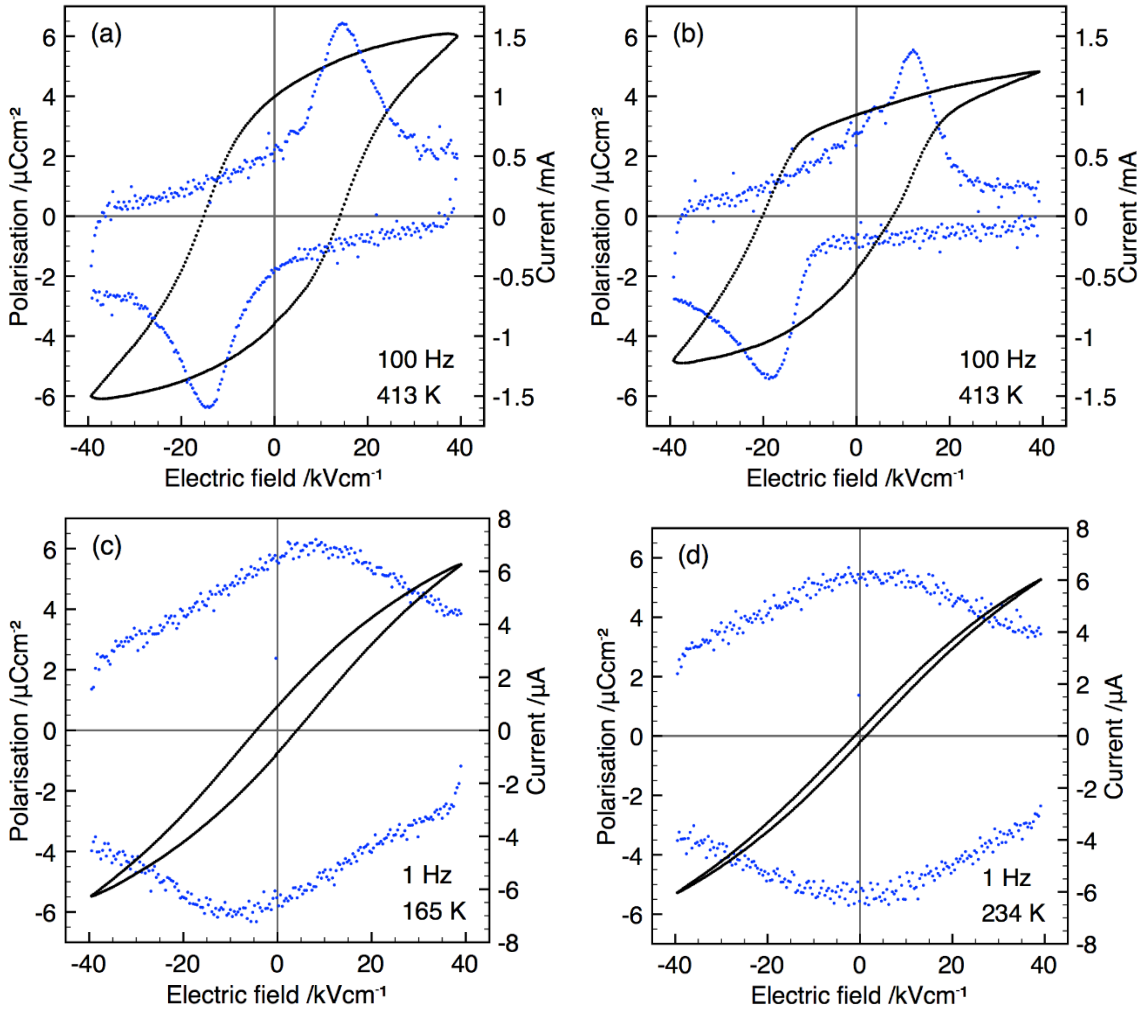

Figure 3. Polarisation-electric field (P-E) loops and associated current-field (I-E) responses for: (a) $x = 0.25$ demonstrating 'normal' ferroelectric switching, (b) x = 0.25 with asymmetric P-E loop; P-E and I-E data for x = 3 showing ferroelectric switching at 165 K (c), and "slim" relaxor-like loop at 234 K (d).